ADVANCED LUMINESCENCE IMAGING OF CIGS SOLAR CELLS

Tetiana Lavrenko, Francillina Robert Runai, Yue Wang, Marcel Teukam, Thomas Walter,
University of Applied Sciences Ulm, Albert-Einstein-Allee 55, 89081 Ulm, Germany
Thomas Hahn (now with Bosch CISTECH)
Paul Pistor, Helmholtz-Zentrum Berlin für Materialien und Energie,
Hahn-Meitner Platz 1, 14109 Berlin, Germany

ABSTRACT: The importance of CIGS-based solar cells for terrestrial application increases steadily. A key issue for a high production yield are efficient inspection tools at the early stage of the production process. The present contribution focuses on imaging characterization of CIGS solar cells including photo- and electroluminescence. PL imaging does not need electrical contacts and can be applied after the absorber deposition prior to the TCO deposition and the completion of the module. The effect of heat treatment on thermally evaporated In_2S_3 buffer layer with respect to the device performance is studied on the "absorber&buffer" stack by PL-imaging. The correlation between PL intensity with achieved open circuit voltages of the completed devices has been established. It will be concluded that the quality of the buffer layer and the interface is well-detectable at this early stage by PL-imaging. The other issue addressed in this contribution is a characterization of graded gap absorbers by EL imaging. It will be demonstrated that luminescence imaging using optical bandpass filters can be used for the evaluation of the bandgap grading of CIGS absorbers fabricated by sequential processes. Furthermore, lateral inhomogeneities with respect to the In/Ga intermixing can be detected already after the absorber deposition by the proposed PL imaging method.
Keywords: CIGS, In_2S_3, Photoluminescence, Electroluminescence

1 INTRODUCTION

CIGS-based solar cells, being the most efficient among all the thin film technologies, exhibit a huge potential for future. High efficiency on a 30x30cm²-sized CIS-based thin film submodule has been achieved by improving uniformity across respective layers [1] Therefore, a key issue for a high production yield are effective inspection tools at the early stages of a fabrication. Luminescence techniques, such as photo- and electroluminescence, have already proven their usefulness for material and device characterization both at the laboratory level and industrial manufacturing. But, nevertheless, their potential usage still can be advanced further.

A quality control of Cd-free buffer layers and the corresponding interfaces proved to be a promising application for PL imaging. The effect of post deposition heat treatment at different temperatures on the evaporated In_2S_3-buffer layers studied by means of PL imaging will be discussed. The PL intensity depends on the splitting of quasi-Fermi levels and, as it will be shown in this paper, correlates to the achieved open circuit voltage of the completed device.

CIGS absorbers fabricated by sequential processes tend to – depending on the fabrication process – segregate in a layer at the back contact with a high Ga content and a layer close to the heterointerface with a low Ga (therefore high In) content [2]. This intermixing of In and Ga can be detected by EL imaging as the emission wavelength is dominated by the lowest bandgap energy.

2 MEASUREMENT SETUP AND MEASURING PRINCIPLE

The luminescence intensities have been captured by an InGaAs camera. The two LED arrays (λ=630 nm) were used to stimulate the PL signal from the CIGS absorber. For EL imaging, various filters with different center wavelengths, mounted directly in front of the camera lens were used to obtain additional spectral information. The schematic drawing of the measurement setup and its photograph are shown in Figure 1 and 2 respectively. The IV-measurements were performed on a Keithley semiconductor analyzer. All measurements were taken at room temperature.

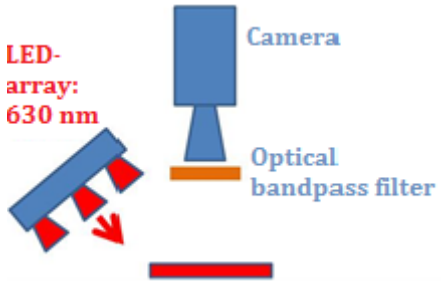

Figure 1: Schematic drawing for luminescence imaging setup.

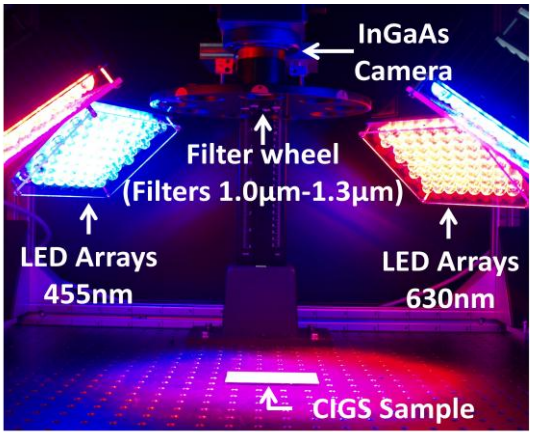

Figure 2: Photo of luminescence imaging setup

3 RESULTS OF SPECTRAL LUMINESCENCE IMAGING

3.1 Determining the spectral emission with spectral EL

In order to validate this concept EL images using these optical bandpass filters were captured and compared to measurements of the emission spectrum with a spectrum analyzer. Figure 3 shows results from two different CIGS solar modules. For sample 1 the emission ranges between 1.0 µm and 1.1 µm as can be deduced from the intensity of the captured images through the filters. Sample 2 indicates a higher emission wavelength from a bandgap close to pure $CuInSe_2$. Figure 3 also shows a comparison of these filter measurements with the emission spectra obtained from an Anritsu spectrum analyzer. As can be deduced from Figure 3 a close agreement exists between these measurements verifying the concept proposed in this contribution.

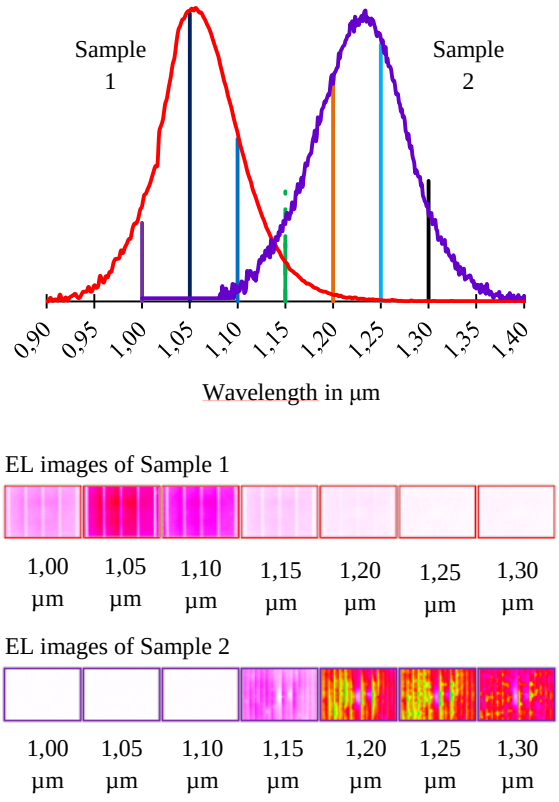

Figure 3: Filter measurements from the EL images (below) are compared with the emission spectra from a spectrum analyzer.

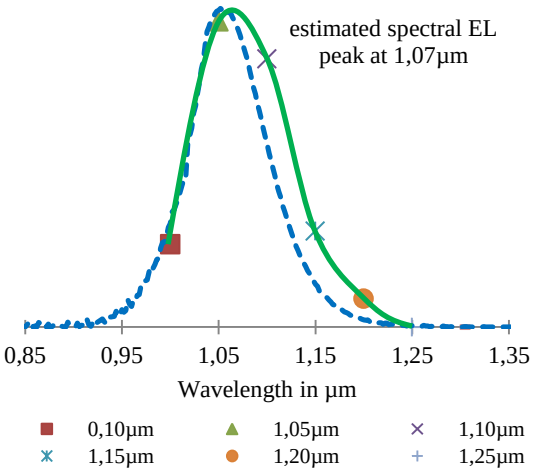

Figure 4: The dashed curve represents the spectral emission of a standard sample while each marking point represents the EL intensity obtained from various optical bandpass filters.

3.2 Determining the peak emission wavelength with a colored glass filter RG9

As spectral EL measurements with optical bandpass filters take roughly 20 minutes, we developed an approach using a single Schott colored glass filter RG-9. This optical filter exhibits a steadily decreasing (well determined) transmission in the wavelength range of interest. Therefore the ratio of the measured EL intensity obtained with and subsequently without filter depends on the emission wavelength. Or in other words – the wavelength information is transformed into an intensity information. There are various methods to extract the wavelength information from intensity measurements using calibrated wavelength dependent transmission filters. A method which is also suitable for multiple filters is the cross correlation between the measured intensities and the calibrated transmission curves. A detailed description and discussion on this method will be published later.

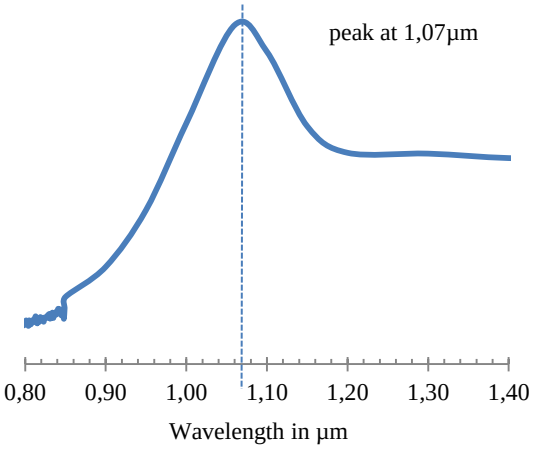

Figure 5: The cross correlation peak value at 1,07µm represents the spectral emission wavelength of the sample determined by EL with a RG-9 filter measurement.

Figure 5 shows the cross correlation of the EL measurement performed on the CIGS module used in Figure 4. This cross correlation indicates a dominant

emission wavelength of 1.07 µm which agrees with the value from spectral EL measurements with optical bandpass filters in Figure 4. This method can be applied to each pixel of an EL image, thus offering the advantage to yield spectral information for EL images. Spectral measurements using a spectrum analyzer determines only a small point of the sample whereby the sample measured with spectral EL in Figure 4 was a 5cm x 5cm mini module sample.

3.3 Application of reciprocity relation between photovoltaic quantum efficiency and EL emission for graded gap absorbers

In the following it will be demonstrated that the reciprocity relation between photovoltaic quantum efficiency and electroluminescent emission [3] is also applicable to graded gap absorbers resulting in a fairly broad spectral EL emission. Therefore, a CIGS absorber fabricated by sequential processes is evaluated and characterized with grazing incidence X-ray diffraction (GIXRD) and external quantum efficiency (EQE) measurements.

GIXRD in conjunction with a modeling algorithm is a powerful tool for studying the structural properties of polycrystalline thin films [4] yielding a structural depth profile. The GIXRD scans in Figure 6 exhibit different structural and therefore compositional depth profiles at the center area compared to the border area of a 30cm x 30cm sub-module as a consequence of a Ga/(In+Ga) distribution depending on the depth. In Figure 7, the resulting Ga/(Ga+In) depth profile derived from GIXRD measurements from the center exhibits a rather homogeneous Ga distribution in the absorber. However, at the border of the module the Ga/(Ga+In) depth profile demonstrates an inhomogeneous Ga-distribution whereby close to the back contact the composition is almost pure $CuGaSe_2$ and close to the heterointerface the composition is almost plain $CuInSe_2$. Further details of the characterization of this particular sample have been elaborated elsewhere [2]

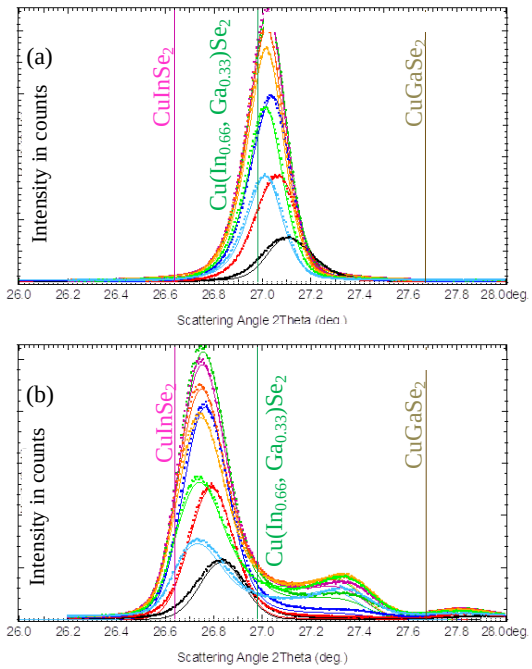

Figure 6: (a) GIXRD scan at the center area (b) GIXRD scan at the border area.

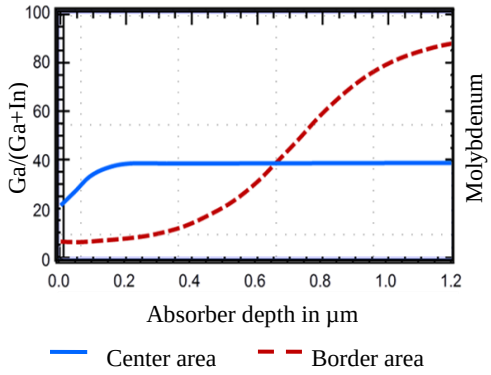

Figure 7: Ga/(Ga+In) depth profile derived from GIXRD scans in Figure 6.

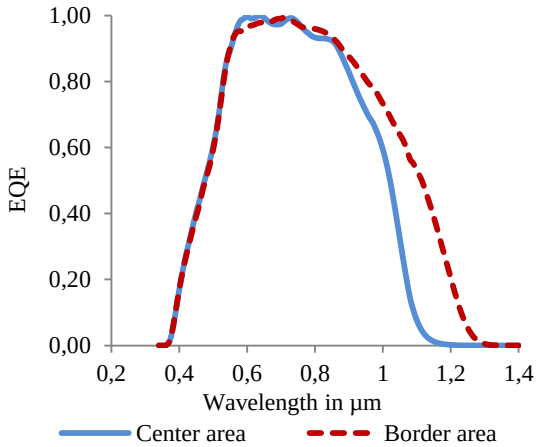

Figure 8: EQE from areas with different compositional depth profiles

The Ga/(Ga+In) ratio also affects the optical band gap [5]. This can be seen from the quantum efficiency measurements in Figure 8. For the absorber with a rather homogeneous Ga distribution in depth a rather sharp onset of the EQE can be observed around 1.1 µm whereas for the graded gap structure the EQE extends to about 1.3 µm corresponding to the bandgap of (almost) pure $CuInSe_2$. According to the reciprocity theorem such a difference in the absorption (EQE) spectrum should correspond to a change of the spectral emission spectrum [3]. From the measured EQE in Figure 8, the emission spectrum was calculated according to the reciprocity relation and compared to the measured EL emission spectrum (Figure 9).

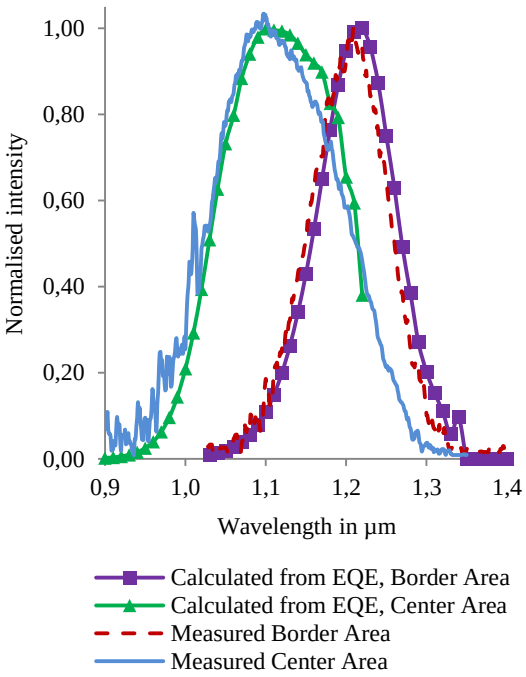

Figure 9: Spectral emission: measured vs. calculated from EQE

From Figure 9 a good agreement between the measured and calculated (from EQE) EL emission spectrum can be deduced. Two consequences should be pointed out: The graded gap structure of the absorber (which determines the solar cell performance to a large extend) is also reflected in the EL emission spectrum. Therefore, a quality control of the bandgap grading could be based on the emission spectrum. The spectral imaging method developed and discussed in the preceding section could be a valuable and fast imaging tool to assess the bandgap grading especially with respect to lateral inhomogeneities.

4 RESULTS FROM EVAPORATED In_2S_3-BUFFER LAYER

A promising candidate for alternative Cd-free buffer layers is thermally evaporated In_2S_3. The efficiency of such devices approached very closely nowadays employed CdS-buffered counterparts [6]. But an industrial implementation of any technology is determined not only by high efficiencies of the devices, but also by a feasibility of its technological process. Thus, optimization of the deposition process of In_2S_3-buffer layer is of great importance to make it competitive with other Cd-free candidates.

The studied CIGS devices with In_2S_3 buffer layers have been supplied by Helmholtz-Zentrum Berlin (HZB) in the framework of the "NeuMaS-Project". These devices had not undergone any post-deposition treatment and will be referred to as "as-grown state". The deposition of the In_2S_3-film has been performed at HZB in accordance with its baseline process. For an optimal performance, these devices have to be annealed at 200°C for 35-45 min. [6]

One of the issues related to the evaporated In_2S_3-buffer layers is to better understand the post-annealing effect and then to eliminate or shorten this step. To investigate the influence of different temperatures on the performance of the tested samples three temperatures 150°C, 200°C and 250°C were chosen.

PL imaging was performed on the samples with absorber and buffer, but without window layer. (For simplicity of writing this type of the samples will be called "absorber&buffer" stack.) Obviously, the Voc measurements were carried out on the completed devices. The objective of the experiment is to show that PL imaging can be applied to predict the photovoltaic performance of the devices as early as directly after buffer layer deposition, with no need to complete the device.

For each device and "absorber&buffer" stack, annealed at the same temperature, Voc and PL intensity measurements were taken each 10 min within 1h. Afterwards, the averaged PL intensity of the "absorber&buffer" stack was compared to the Voc of the corresponding device. The results for different annealing temperatures over the annealing time are shown in Figure 10.

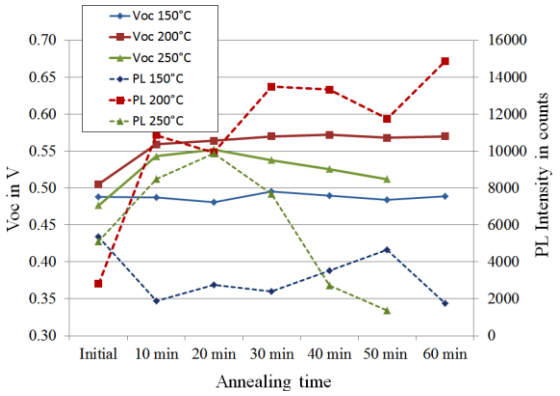

Figure 10: Development of Voc of the completed devices (solid line) and PL intensity of the "absorber&buffer" stack (dashed line) at 150°C, 200°C and 250°C.

As can be seen from Figure 10, annealing at 150°C does not have a significant effect on the performance of the tested samples. Both Voc and PL intensity exhibit just slight parameter drifts. A different trend is observed for annealing at 200°C. A significant increase of the PL intensity and Voc is already detected after 10-15 min of heat treatment followed by a stabilization of these values. This temperature has the most beneficial effect among the three. After annealing at 250°C an increase of Voc and PL intensity is followed by a fast drop of these parameters.

4.1 Discussion on Annealing Effect

Based on results of our experiments, it is clear that the temperature during the annealing has a crucial effect on the performance of the solar cells with an In_2S_3 buffer layer. The samples annealed at 150°C showed minor changes in both PL intensity and Voc values. This temperature is too low to affect in any way the properties of the heterojunction. After annealing at 200°C the tested samples have been found significantly improved with respect to Voc for the completed devices and PL intensity for the "absorber&buffer" stack. This improvement can be attributed to Cu-diffusion from the absorber to the In_2S_3 layer [7], [8]. The Cu-atoms occupy vacancies and some of the In-sites in the In_2S_3 layer, leaving behind a Cu-poor layer at the absorber side. [8] Thus, air-annealing leads to the formation of a compositionally

graded In_2S_3/CIGS interface which, by-turn, is responsible for the improvement of the performance of these devices [7] by a transition from an interface dominated recombination to a bulk dominated recombination. Since PL intensity also increases, it is appropriate to mention here that annealing reduces the non-radiative recombination at the interface resulting in an increased PL intensity (for a constant generation rate). Annealing at 250°C has an opposite effect. This temperature is too high and leads to a deterioration of the studied parameters. After an initial increase of the PL intensity and Voc, a fast drop afterwards is observed. As has been stated in [7], a $CuIn_5S_8$-phase formation can be a reason for the deterioration of the properties of the heterojunction. This interfacial layer has a large density of defects and vacancies which provide a large number of recombination centers and, thus, provokes a bad solar cell performance.

These results prove that the effect of each temperature can be explicitly identified either on the completed devices by measuring Voc or on the "absorber&buffer" level by taking PL images. Since these two parameters show a strong correlation it follows that PL-imaging can be applied at the early stage of production process to predict the quality of the outgoing devices.

5 CONCLUSIONS

Luminescence characterization of CIGS solar cells has already proven its usefulness for laboratory level research and quality control throughout manufacturing processes. In this contribution new applications of photo- and electroluminescence imaging have been presented and discussed. Bandgap grading as a result of reactive processes affects the emission spectrum as a consequence of the reciprocity theorem. Therefore, spectral PL or EL imaging is a valuable method for the quality control of such devices. We proposed a new and rather simple method for spectral imaging using one or more wavelength dependent transmission filters. This correlation method can be applied on each pixel and consequently allows 2D imaging with spectral information.

The effect of heat treatment at 150°C, 200°C and 250°C on evaporated In_2S_3 buffer layers has been studied by PL-imaging. The correlation between the PL intensity of the "absorber&buffer" stacks and the Voc of the completed devices has been established. Based on the results obtained, it follows that the quality of the CIGS devices with In_2S_3 buffer layers can be already evaluated on the absorber level prior to the completion of the device.

6 REFERENCES

[1] H. Sugimoto, T. Yagioka, M. Nagahashi, Y. Yasaki, Y. Kawaguchi, T. Morimoto, Y. Chiba, T. Aramoto, Y. Tanaka, H. Hakuma, S. Kuriyagawa and K. Kushiya, 37th IEEE PVSC Seattle, 2011.

[2] F. Robert Runai, F. Schwäble, T. Walter, A. Fidler, S. Gorse, T. Hahn and I. Kötschau, 37th IEEE PVSC Seattle, 2011.

[3] U. Rau, Physical Review B76 (2007) 085303-1 - 085303-8

[4] I. Kötschau, G. Bilger and H. Schock, Mat. Res. Soc. Symp. Proc. Vol. 763, 2003.

[5] G. Mount, J. Moskito, U. Sharma, G. Strossman, L. Wang, P. Schnabel, T. Buyuklimanli and K. Putyera, 37th IEEE PVSC Seattle, 2011.

[6] P. Pistor, 27th EU PVSEC, Frankfurt am Main, 2012 to be published at this conference.

[7] D. Abou-Ras, G. Kostorz, A. Strohm, H.-W. Schock, A. N. Tiwari, J. Appl. Phys. 98, 123512 (2005).

[8] P. Pistor, Formation and Electronic Properties of In_2S_3/Cu(in,Ga)Se_2 Junctions and Related Thin Film Solar Cells. PhD thesis, Freie Universität Berlin, 2009.

7 ACKNOLEDGEMENTS

This work has been partly funded by German Federal Ministry of Education and Research.